PHYSICAL REVIEW LETTERS

Ab Initio Analysis of Electron-Phonon Coupling in Molecular Devices

N. Sergueev, D. Roubtsov, and Hong Guo

Center for the Physics of Materials and Department of Physics, McGill University, Montreal, PQ, Canada, H3A 2T8
(Received 6 March 2005; published 29 September 2005)

We report a first principles analysis of electron-phonon coupling in molecular devices under external bias voltage and during current flow. Our theory and computational framework are based on carrying out density functional theory within the Keldysh nonequilibrium Green's function formalism. Using a molecular tunnel junction of a 1,4-benzenedithiolate molecule contacted by two aluminum leads as an example, we analyze which molecular vibrational modes are most relevant to charge transport under nonequilibrium conditions. We find that the low-lying modes are most important. As a function of bias voltage, the electron-phonon coupling strength can change drastically while the vibrational spectrum changes at a few percent level.

PACS numbers: 73.63.−b, 68.37.Ef, 72.10.−d, 81.07.Nb

One of the most important questions concerning charge transport in molecular electronic devices is the role of electron-phonon (e-p) interaction. Here, "phonon" refers to quantized molecular vibrational modes which couple to various scattering states of the device. A typical molecular device has the metal-molecule-metal (MMM) configuration schematically shown in Fig. 1, where metal leads extend too far away and bias voltages can be applied so that a current flows through. The problem of predicting vibrational spectra and e-p coupling strength for such an open system during current flow, within self-consistent first principles including all atomic details of the molecule as well as the leads, is a serious theoretical challenge. A particularly important problem is to understand which vibrational mode couples to which scattering state at what bias voltage [1,2]. It is the purpose of this Letter to address this issue.

Experimentally, single molecule vibrational spectra can be measured by inelastic tunneling spectroscopy (IETS) [3–5]. Theoretically, various models have been applied to understand IETS and to investigate effects of e-p interaction based on tight binding atomistic Hamiltonians [6–8]. Recently, Frederiksen *et al.* [9] reported an important first principles analysis of inelastic current due to e-p interactions in an Au chain, in which the relevant vibrations are along the chain length. In their theory [9], the vibrational spectra was obtained using a plane-wave basis density functional theory (DFT) code in a cluster configuration at equilibrium, and the dynamic matrix was evaluated using a finite differencing scheme. Transport properties were then obtained using the Transiesta package [10] which carries out DFT within the nonequilibrium Green's function (NEGF) formalism, and e-p scattering was included as self-energy into the NEGF at the level of self-consistent Born approximation.

In order to investigate voltage dependence of the e-p interaction in MMM devices, quantized molecular vibrations and electrons need to be treated on equal footing at *nonequilibrium*. We accomplish this by carrying out DFT

atomic analysis within the Keldysh nonequilibrium Green's function (NEGF) formalism [10,11]. Some recent work [12] has put the application of DFT to transport on a more rigorous basis. Time dependent DFT has also been put on a more rigorous basis for analyzing transport problems [13]. Issues concerning the variational principle and quantum mechanical forces at nonequilibrium have been discussed by several authors [14]. In the following, we calculate the dynamic matrix within the NEGF-DFT formalism [11] by evaluating an analytical formula rather than numerical finite differencing [9]: this is more general and more accurate so that all the phonon modes and e-p couplings can be obtained for complicated systems. For a molecular tunnel junction of a 1,4-benzenedithiolate (BDT) molecule contacted by two metallic electrodes (Fig. 1), we found that the low-lying modes of the vibration are the most important for e-p coupling. As a function of bias voltage, the coupling strength can change drastically while the vibrational spectrum changes at a few percent level.

We start from the NEGF-DFT formalism documented in Ref. [11]. After the Kohn-Sham (KS) Hamiltonian $\hat{H}_{KS}[\hat{\rho}]$ of the device is obtained self-consistently, the total energy of the scattering region (Fig. 1), as well as all transport
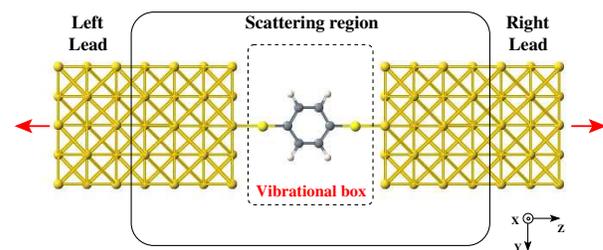

FIG. 1 (color online). Schematic plot of a metal-BDT-metal molecular tunneling junction. The electrodes consist of repeated unit cells extending to $z = \pm\infty$. The scattering region contains several layers of electrodes and the molecule. The vibrational box lies inside the scattering region.

properties of the device, can be obtained [11]. Importantly, the NEGF-DFT formalism allows one to obtain $\hat{H}_{KS}$ and total energy $E(\{\mathbf{R}_i\}, V_b)$ as functions of external bias V_b ($\mathbf{R}_i$ the position of the ith atom). The phonon (vibrational) eigenvectors $\mathbf{e}_\nu$ and frequencies ω_ν (ν is the mode index) are obtained by diagonalizing the dynamic matrix (Hessian matrix) $\mathcal{H}_{j,j'} = \nabla_{\mathbf{R}_j}\nabla_{\mathbf{R}_{j'}}E(\{\mathbf{R}_i\}, V_b)/\sqrt{M_j M_{j'}}$, where M is the mass of an atom. Once $(\mathbf{e}_\nu, \omega_\nu)$ are obtained, the e-p interaction strength g^ν, defined by the e-p Hamiltonian [15], can be obtained from the standard expression $g^\nu_{j,\mu;j',\mu'} = \sum_i \sqrt{\frac{\hbar}{2M_i\omega_\nu}}\mathbf{e}(\nu, i)\langle\phi_{j,\mu}|\nabla_{\mathbf{R}_i}\hat{H}_{KS}|\phi_{j',\mu'}\rangle$. Here, $|\phi_{j,\mu}\rangle$ is a basis function for orbital μ ($\mu = s, p, d$) of the jth atom. The derivative of the KS Hamiltonian is carried out by fixing the atomic positions at their stationary locations $\mathbf{R}_i^0$ ($\mathbf{R}_i^0$ is where the ith atom feels no force). Although the Hessian matrix and $g^\nu_{j,\mu;j',\mu'}$ appear to have the same form as those for equilibrium system, the derivatives of $\hat{H}_{KS}(\{\mathbf{R}_i\}, V_b)$ and $E(\{\mathbf{R}_i\}, V_b)$ with respect to $\mathbf{R}_i$, propagate to derivatives of NEGF that include nonequilibrium physics.

The e-p coupling is characterized by a dimensionless parameter [15] λ_{e-p} which is contributed by all phonon modes,

$$\lambda_{e-p} = \sum_\nu \lambda_\nu, \qquad \lambda_\nu \equiv \text{DOS}(\varepsilon_F)\frac{|\langle g^\nu\rangle|^2}{\hbar\omega_\nu}. \qquad (1)$$

Here, DOS is the density of states of the scattering region and ε_F the Fermi energy of the leads. As we are interested in e-p coupling for quantum transport, the g^ν matrix is averaged over scattering states Ψ_{sc} which are obtained by the NEGF-DFT numerical package [11] for any MMM device:

$$\langle g^\nu(E, E')\rangle = \langle\Psi_{sc}(E)|g^\nu|\Psi_{sc}(E')\rangle. \qquad (2)$$

If both scattering states have the same energy $E = E' = \varepsilon_F$, we call such an e-p coupling the "elastic" one, λ_ν^{el}. When $E = \varepsilon_F$ and $E' = \varepsilon_F \pm \hbar\omega_\nu$, we call it the "inelastic" $\lambda_\nu^\pm$. Finally, when the MMM device is under an external bias voltage V_b, we further average λ_ν over the transport energy window (μ_L, μ_R) where $\mu_{R/L}$ are the electrochemical potentials of the right and left leads and $|\mu_R - \mu_L| = eV_b$. Hence, at nonequilibrium, we obtain

$$\lambda_\nu^{el}(V_b) = \int_{\mu_L}^{\mu_R}\frac{dE}{eV_b}\text{DOS}(E)\frac{|\langle g^\nu(E, E)\rangle|^2}{\hbar\omega_\nu}. \qquad (3)$$

The inelastic coupling $\lambda_\nu^\pm(V_b)$ is calculated by replacing $g^\nu(E, E)$ with $g^\nu(E, E \pm \hbar\omega_\nu)$ in Eq. (3).

In numerical calculations, we further define a "vibrational box" inside the MMM device (Fig. 1) which contains the atoms whose vibrational properties are of interest. In the following, we investigate general features of vibrational spectra and e-p coupling during nonequilibrium transport using the model MMM device of Fig. 1 as an

example, i.e., a BDT molecular wire. In the model calculation, the two identical Al leads contact the BDT by a distance of 2 Å. The leads have a finite cross section oriented in the (100) direction with nine atoms per unit cell and extend to $z = \pm\infty$. The vibrational box includes the molecule. A single zeta s, p, d basis set is used in the NEGF-DFT self-consistent calculations. For each bias voltage, we iterate the KS Hamiltonian of the device to numerical convergence using the NEGF-DFT method [11]; the atomic positions in the scattering region must also be relaxed for each applied bias. Afterward, the vibrational spectrum and the e-p coupling are obtained. As a check, we calculated ω_ν of an isolated BDT using our NEGF-DFT formalism and obtained reasonable agreement, to within $\leq$5%–6%, with experimental data collected by Raman spectroscopy and other methods [16]. We also checked that the *diagonal* matrix elements of the e-p coupling are nonzero for modes having the A_g symmetry and are zero for other modes, in agreement with selection rules from group theory [17].

When the BDT is placed between the leads (Fig. 1), new properties arise. First, several low-lying modes that do not exist for isolated BDT are found to play important roles. These modes include the center of -mass and libration [c.m. (i) and LB (i), $i = X, Y, Z$] with energy $\hbar\omega_\nu \simeq$ 8–14 meV. Clearly, the presence of leads breaks the translational and rotational symmetries and produces these low-lying modes. Second, many vibrational frequencies are renormalized, to $\simeq$ 10%–30%, from that of the isolated molecule. This is especially true for modes with strong sulfur oscillations in the BDT. For large bias, $V_b \approx 1$ V, we found that ω_ν changes up to 2% while $\mathbf{e}_\nu$ changes up to
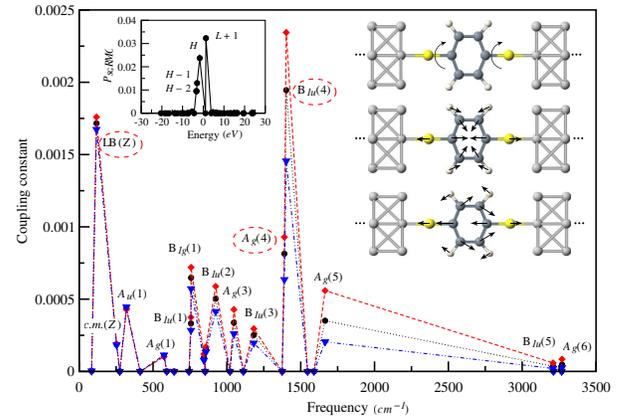

FIG. 2 (color online). Dimensionless e-p coupling constants λ_ν^{el} (circles), λ_ν^- (triangles), λ_ν^+ (diamonds) as a function of vibrational frequency ω_ν at $V_b = 0$. The lines are guides to the eye. The modes are classified using the D_{2h} point group. The left inset shows a projection $P_{sc,RMO}$ of a scattering state at Fermi energy (shifted to zero). Letters H and L mean HOMO and LUMO. The right-side insets show eigenvectors of several important eigenmodes of the BDT at small biases: the LB (Z), top; A_g(4), middle; and B_{1u}(4), bottom.

5% compared with the vibrational spectrum at $V_b = 0$. At $V_b = 0$, it turns out that all the modes can be classified by the same D_{2h} point group as in the case of an isolated BDT; at $V_b \neq 0$, they can be classified by the C_{2v} point group.

Figure 2 plots the e-p coupling λ_ν versus $\hbar\omega_\nu$ at $V_b = 0$. For small bias voltages, $V_b \lesssim 0.5$ V, λ_ν does not change qualitatively. Most clearly shown is that some phonon modes give distinctly larger e-p coupling to scattering states than others [see Eq. (2)]. Beside the expected in-plane $A_g(n)$ modes, modes of other symmetries are also responsible for the peaks in λ_ν (see the right insets of Fig. 2 for a few important modes). Notable are the in-plane modes $B_{1u}(n)$, out-of-plane modes $A_u(n)$, and modes c.m. (Z) and LB (Z). Recall that for vibrational spectroscopy on free BDT such as Raman or infrared, there are always selection rules of modes [16]. For a BDT device, however, our results suggest that no obvious selection rules are followed because many modes with very different symmetries manifest. Interestingly, among the low-lying modes with $\omega_\nu < 1000$ cm^{-1} ($\hbar\omega_\nu < 0.12$ eV), the "breathing" modes $A_g(1)$ and $A_g(2)$ are not the most important ones for coupling to scattering states ($\lambda_\nu \simeq 1$–2×10^{-4}), although these modes are important for a free BDT. For the BDT device, the total e-p coupling [Eq. (1)] is $\lambda_{e\text{-}p}^{\text{el}} \approx \lambda_{e\text{-}p}^{-} \approx 7 \times 10^{-3}$ at $V_b = 0$.

To understand why modes with symmetry other than A_g can couple to scattering states (Fig. 2), we consider Eq. (2). For a *free* BDT, the electronic wave function is a molecular orbital, for each orbital one obtains a value $\langle g^\nu \rangle$, thus the relevant e-p coupling is a diagonal matrix and only those vibrational modes with A_g symmetry give nonzero values to $\langle g^\nu \rangle$ [17]. For transport, however, the wave function appearing in Eq. (2) is a scattering state which is roughly a linear combination of many molecular orbitals. Therefore it is possible to have off-diagonal matrix elements in the coupling matrix so that modes with symmetries other than A_g can also contribute. This can be substantiated by projecting scattering states $\Psi_{\text{sc}}(E)$ onto "renormalized molecular orbitals" (RMO) of the BDT [18]. RMO's are obtained by diagonalizing the Hamiltonian submatrix that corresponds to the BDT molecule of the MMM device [18]; RMO's can be different from molecular orbitals of an isolated BDT due to charge transfer from the leads to the molecule and external bias potentials. The projection is characterized by the quantity $P_{\text{sc,RMO}} \equiv |\langle \Psi_{\text{sc}}(\varepsilon_F)|\text{RMO}\rangle|^2$ plotted in the left inset of Fig. 2 as a function of energy. We found that all scattering states Ψ_{sc} near the Fermi energy are contributed by the *same several* dominant RMO's at low bias. Therefore one can well consider that Ψ_{sc} is a linear combination of these few RMO's and g^ν of Eq. (2) is contributed mostly by them; i.e., $\langle g^\nu \rangle$ is contributed by a quantity $g^\nu_{\alpha\alpha'} \equiv \langle \text{RMO}_\alpha | g^\nu | \text{RMO}_{\alpha'} \rangle$. Hence, for transport problems, the off-diagonal contributions (when $\alpha \neq \alpha'$) can be as important as the diagonal ones ($\alpha = \alpha'$). Furthermore, when

bias V_b is increased, molecular orbitals in the MMM device [18] become less symmetric so that vibrational modes different from the A_g symmetry can even contribute to the diagonal matrix elements of the e-p coupling. For example, at $V_b = 1$ V, the contribution of orbitals HOMO-n with $n = 1, 3$ to the scattering states is found to give rise to nonzero e-p coupling for vibrational modes with both the A_g and B_{1u} symmetries. This shows that e-p coupling in MMM devices during current flow ($V_b \neq 0$) is more complicated than that for free molecules.

A most important finding is that at larger bias voltage, $V_b \simeq 1$ V, the e-p coupling strength changes drastically although the vibrational spectrum is only changed by a few percent as mentioned above. Figure 3 plots the coupling strength at $V_b = 1$ V. We observe that contributions to e-p coupling are now dominated by a few low-lying modes such as the center-of-mass modes; the total coupling is a factor of 5 greater than that at low bias (Fig. 2); and coupling due to individual low-lying modes is also much larger. By projecting different scattering states $\Psi_{\text{sc}}(E)$ with the same energy E onto RMO's as presented above, we found that two patterns of $P_{\text{sc,RMO}}(E_{\text{RMO}})$ occur, as shown in the left insets of Fig. 3. This indicates that scattering states inside the transport energy window are different from those at low bias. In particular, the pattern of $P_{\text{sc,RMO}}$ in the upper panel is similar to that in Fig. 2, but the new (lower) pattern of $P_{\text{sc,RMO}}$ comes from lower HOMO-n and higher LUMO + n RMO's. This leads to a different behavior of e-p couplings at larger biases for the BDT device. For example, our calculations reveal that the peak labeled c.m. (Y) in $\lambda_\nu(\omega_\nu)$ (Fig. 3) comes from particular off-diagonal matrix elements, $\langle L + 2|g^\nu|H - 1\rangle$ and $\langle L + 4|g^\nu|H - 1\rangle$. The peak labeled c.m. (Z), on the other hand, is found to come from diagonal matrix ele-
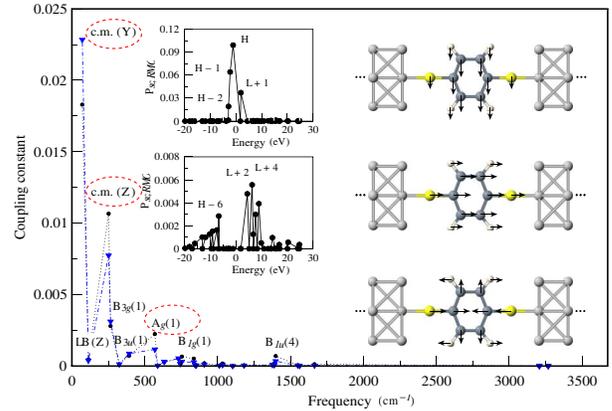

FIG. 3 (color online).   Coupling constants λ_ν^{el} (circles) and λ_ν^{-} (triangles) at $V_b = 1$ V. Although in principle one should use the C_{2v} point group to label the modes, for comparison with Fig. 2 we keep the D_{2h} labels. The left insets show projection $P_{\text{sc,RMO}}$ for two scattering states taken at $E - \varepsilon_F = 0.4$ eV. The right-side insets show eigenvectors of several important modes at $V_b \simeq 1V$: c.m. (Y), top; c.m. (Z), middle; and $A_g(1)$, bottom.
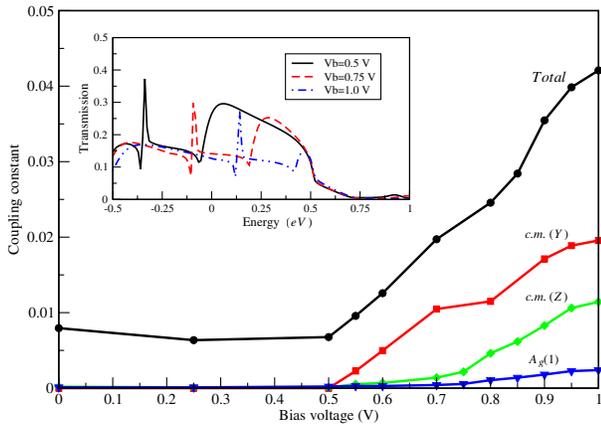
FIG. 4 (color online). Coupling constants $\lambda^{\mathrm{el}}_{e\text{-}p}$ (circles) and $\lambda^{\mathrm{el}}_\nu$, for $\nu =$ c.m. (Y) (squares), c.m. (Z) (diamonds), and $A_{\mathrm{g}}(1)$ (triangles), as a function of V_b. Inset: transmission function $T(E, V_b)$ at $V_b = 0.5$ (solid line), 0.75 (dashed line), and 1 V (dashed-dotted line). The transport energy window lies from $E = 0$ to $E = |eV_b|$.

ments, e.g., $\langle H - 1|g^\nu|H - 1\rangle$. These findings also correlate well with the peaks of $P_{\mathrm{sc,RMO}}$ in the left insets of Fig. 3. The total $\lambda_{e\text{-}p}$ at $V_b \simeq 1$ V is found to be $\simeq 0.04$. This enhancement by roughly a factor of 5 from that of $V_b \simeq 0$ is due to the center-of-mass modes shown in Fig. 3 which can be confirmed by computing $\lambda_{e\text{-}p}$ without counting these modes.

Why can bias voltage change $e\text{-}p$ coupling so drastically? We found that the reason is mainly due to the contribution of different scattering states. In the inset of Fig. 4, we plot the transmission coefficient $T(E, V_b)$ vs electron energy E for several values of V_b. Most clearly shown is that V_b shifts the transmission features toward the transport window. In particular, a sharp peak (at $E \approx -0.3$ eV) is shifted upwards in energy with the increase of V_b. When $V_b > 0.5$ V, the "tail" of this sharp peak starts entering the transport window [between $\mu_L = 0$ and $\mu_R = eV_b$, see also Eq. (3)]. When $V_b > 0.75$ V, this peak enters into the transport window completely. When this happens, the $e\text{-}p$ coupling changes drastically and the new pattern appears in the projection $P_{\mathrm{sc,RMO}}$ as discussed above. Figure 4 plots the $e\text{-}p$ coupling strength λ_ν for several vibrational modes ν and the total $\lambda_{e\text{-}p}$ vs V_b. The curves give a clear indication that the $e\text{-}p$ coupling is roughly a constant at small biases, but can change *nonlinearly* as the applied bias voltage is varied. We believe a V_b dependence of $e\text{-}p$ coupling strength should be rather general for other molecular wires even though the details may differ from that of the BDT wire. Such a change can have deep implications to local heating in the device during nonequilibrium charge transport [6,9,19].

In summary, the entire relevant vibrational spectrum of a molecular device can be obtained at nonzero bias within the NEGF-DFT formalism where both vibrational and electronic properties are calculated at equal footing. For the 1,4-BDT molecular device example, low-lying vibrational modes play an important role in contributing to the $e\text{-}p$ coupling strength which changes drastically as bias voltage is increased due to participations of new scattering states. The vibrational spectrum also depends on bias, but for the BDT device this dependence is at a few percent level. Finally, we point out that the bias dependent $e\text{-}p$ interaction studied here can be used to analyze the physics of inelastic current applying, for example, the self-consistent Born approximation as that of Refs. [7,9].

[1] N. Lorente and M. Persson, Phys. Rev. Lett. **85**, 2997 (2000); N. Lorente *et al.*, *ibid.* **86**, 2593 (2001).
[2] M. J. Montgomery *et al.*, J. Phys. Condens. Matter **15**, 731 (2003).
[3] W. Ho, J. Chem. Phys. **117**, 11 033 (2002).
[4] W. Wang, T. Lee, I. Kretzschmar, and M. A. Reed, Nano Lett. **4**, 643 (2004).
[5] Y. Selzer *et al.*, Nano Lett. **5**, 61 (2005).
[6] M. J. Montgomery and T. N. Todorov, J. Phys. Condens. Matter **15**, 8781 (2003).
[7] M. Galperin, M. Ratner, and A. Nitzan, J. Chem. Phys. **121**, 11 965 (2004).
[8] Y. Asai, Phys. Rev. Lett. **93**, 246102 (2004).
[9] T. Frederiksen *et al.*, Phys. Rev. Lett. **93**, 256601 (2004).
[10] M. Brandbyge *et al.*, Phys. Rev. B **65**, 165401 (2002).
[11] J. Taylor, H. Guo, and J. Wang, Phys. Rev. B **63**, 245407 (2001).
[12] X. Zheng and G. Chen, physics/0502021.
[13] G. Stefanucci and C.-O. Almbladh, Europhys. Lett. **67**, 14 (2004); M. Di Ventra and T. N. Todorov, J. Phys. Condens. Matter **16**, 8025 (2004).
[14] T. N. Todorov, J. Hoekstra, and A. P. Sutton, Philos. Mag. B **80**, 421 (2000); M. Di Ventra and S. T. Pantelides, Phys. Rev. B **61**, 16 207 (2000); M. Di Ventra, Y.-C. Chen, and T. N. Todorov, Phys. Rev. Lett. **92**, 176803 (2004).
[15] O. Gunnarsson, Rev. Mod. Phys. **69**, 575 (1997).
[16] S. H. Cho *et al.*, J. Phys. Chem. **99**, 10 594 (1995); S. W. Joo, S. W. Han, and K. Kim, J. Colloid Interface Sci. **240**, 391 (2001).
[17] M. Tinkham, *Group Theory and Quantum Mechanics* (McGraw-Hill, New York, 1964).
[18] B. Larade *et al.*, Phys. Rev. B **64**, 195402 (2001).
[19] Y.-C. Chen, M. Zwolak, and M. Di Ventra, Nano Lett. **3**, 1691 (2003); **4**, 1709 (2004); Z. Yang *et al.*, Phys. Rev. B **71**, 041402 (2005).